Doctoral research plan

Submission date: 30/01/2008

Presented by: Moshe Biton

Supervisor: Prof. Yinon Ben-Neriah

Regulation of the Wnt signaling pathway and maintenance of gut homeostasis by microRNAs

בקרה של מסלול הכוונת אותות Wnt ושמירה על הומאוסטזיס המעי על-ידי microRNAs

I hereby approve the subject and research plan, and agree to guide the student in this work.

Prof. Yinon Ben-Neriah

Summary

The conserved Wnt/β-Catenin signaling pathway plays a crucial role in both cellular proliferation and embryonic development. This pathway has also a key role in the maintenance of homeostasis in the gut, where rapid cellular turnover is taking place throughout the life of vertebrate organisms. Deregulation of this pathway is implicated in driving the formation of various types of human cancers, in particular colorectal cancer. In 80% of these tumors, mutations are found in the Wnt negative regulator and tumor suppressor gene, adenomatous polyposis coli (APC). These mutations lead to the accumulation of β-catenin and consequently to aberrant activation of the Wnt pathway.

Recently, microRNAs have emerged as novel regulators of gene expression. These small molecules suppress or activate gene expression through the RNAi machinery, where microRNA binds to complementary messenger RNA (mRNA) and affects its translation. MicroRNAs are known to participate in vast biological processes, including development, cell-proliferation, apoptosis and tumorgenesis. Most microRNA molecules serve as fine-tuning regulators of gene expression. However, regulation by microRNAs may influence the overall signal and lead to dramatic effects. Based on this general knowledge, we speculated that microRNAs may be involved in the regulation of the Wnt/β-catenin signaling pathway.

To explore this theory, several different approaches were taken. First, a computer based genomic search was conducted to determine if Wnt signaling regulates microRNAs. Using this approach, a specific set of microRNAs harboring Wnt responsive elements were discovered, such as the miR-103 family. By over-expressing miR-103 in human colorectal cell lines (CRCs), we found that following Wnt stimulation, these microRNAs control the level of the Wnt negative regulator, Axin2. Second, we examined the effects of microRNA biosynthesis inhibition on Wnt signaling, by silencing one of the key players of the RNAi machinery-Drosha, in different CRCs. Preliminary results indicate, that under the inhibition of mature microRNAs, β-catenin levels are higher and the Wnt signal is prolonged. Third, we have generated a gut epithelium conditional and inducible Dicer knockout mouse. Dicer is an RNase III-like enzyme crucial for microRNA biogenesis. In these mice we aim to investigate the role of microRNAs in intestinal epithelial cells development and homeostasis. Interestingly, the deletion of mature microRNAs in the gut of adult mice revealed both immunological and differentiation defects. Currently, we are in the process of investigating and understanding the underlying mechanisms of this unique phenotype. These abnormalities could be explained, not only by Wnt dependent phenomena, but also by the complex signaling network regulated by microRNA.

Introduction

The canonical Wnt pathway

The canonical Wnt pathway is a conserved signal transduction cascade which plays a critical role in cell differentiation and regeneration during embryonic development and stem cell maintenance/renewal in adult tissue[1-3]. Signaling is initiated when Wnt ligands bind their associated receptor complex, consisting of a serpentine receptor of the Frizzled family and a member of the LDL receptor family, Lrp5/6 [4]. The central player in the canonical Wnt signaling cascade is the transcription co-activator, β- catenin, whose stability is regulated by a cytoplasmic protein complex called the destruction complex[1,2]. The β-catenin destruction complex is composed of two tumor suppressor scaffold proteins, Axin and adenomatous polyposis coli (APC) and two kinases, CKI and GSK3. In the absence of a Wnt signal, Axin and APC bind newly synthesized β-catenin, leading to the phosphorylation of conserved Ser and Thr residues in the amino terminus of β-catenin by CKI and GSK3[5]. This phosphorylation event recruits the β-TrCP/SCF E3 ubiquitin ligase, which targets β-catenin for proteasomal degradation. Binding of the Wnt ligand to its receptor inhibits the kinase activity of the destruction complex by a poorly understood mechanism, which on the basic level includes removal of Axin from the destructive complex and consequently leads to the accumulation of β-catenin in the cytoplasm. Significantly, β-catenin accumulates and translocates into the nucleus where it associates with DNA-binding proteins of the Tcf/Lef family [6]. The Tcf/Lef proteins are part of the High-Mobility-Group (HMG) transcription factor proteins. The vertebrate genome encodes four highly similar Tcf/Lef proteins, which bind to consensus sites within the genome [7]. In the absence of a Wnt signal, Tcf/Lef proteins repress Wnt target genes through a direct association with transcriptional co-repressors such as Groucho [8]. The interaction with β-catenin transiently converts Tcf/Lef factors into transcriptional activators that in turn initiate the transcription of Wnt target genes, such as Axin2, Cyclin-D1 and c-Myc. The activation of specific target genes set the cellular programming of the Wnt signal. Interestingly, a classical Wnt target gene is Axin2 which is known to play a role as a negative regulator in the Wnt pathway [9,10].

In short, multiple layers of regulation including transcriptional activation, protein modifications, protein localization and protein degradation control the Wnt signaling pathway activation. With the expanding world of m microRNAs one would expect that these novel regulatory molecules will also play a role in a major developmental signaling pathway such as the Wnt pathway and indeed, it has recently been reported that miR-315 regulates Axin1 and Notum in drosophila [11].

Deregulation of the canonical Wnt signal leads to various types of cancer, among them colorectal carcinoma (CRC), melanoma and hepatocellular carcinoma (HCC). In such cancers one or more Wnt components is mutated, resulting in aberrant accumulation of nuclear β-catenin [1-3]. More specifically, Wnt pathway abnormal activation is associated with sporadic and inherited colorectal cancer where APC, β-catenin or Axin2 mutations are found.

The Wnt signaling play a role in some self-renewing tissues, such as the intestinal tract, and remains essential throughout life. The Wnt cascade is the dominant force in controlling cell fate along the crypt-villus axis. Mainly, the Wnt signaling is required for the establishment and proliferation of gut epithelium progenitor cells. Mutations in the Wnt pathway tip the homoeostatic balance in these tissues to cause pathological conditions including cancer [1,2,12].

The Intestinal Tract

The intestinal tract acts as a good mammalian model for the study of tissue self-renewal. The basic tissue architecture of the mouse intestine is established during mid to late gestation in the womb [13]. Around the third week of life, proliferate pockets invade into the submucosa to form mature crypts of Lieberkühn [14]. In the newly formed as well as the adult gut, new cells proliferate in the crypts and migrate toward the villi tips where they are later removed by apoptosis [15]. Only the epithelial stem cells and Paneth cells (fully differentiated) escape this flow and remain positioned at the crypt's base [16]. The epithelial stem cells self-renew throughout an animal's life, cycling infrequently to produce proliferating cells that fill the remainder of the crypts. Stem cells and Paneth cells of the small intestine (SI) occupy positions +1 to +4 of the crypt base [1,17]. In the colon, Paneth cells are absent, and the stem cells reside directly at the base of the crypt [18].

The intestinal tissue poses a barrier between the body and the outside world. The intestinal epithelium consists of single layer epithelial cells. These cells absorb vital nutrients while keeping indigestible bulk and associated microflora inside the lumen. In order to distinguish between pathogenic antigens and normal antigens, the intestine epithelial cells (IECs) adopted several immunological traits [19-24]. Among these traits, they express sensor-like molecules such as the MHC class I and II (self and non-self), special effectors against a range of pathogens (antibacterial substrates), and mucus to prevent pathogen adhesion [25]. Recently, a crosstalk between IECs and the innate and adaptive immune system was revealed [19,20,24]. It has been suggested that IECs have a crucial immune function in protection and maintenance of gut homeostasis. Interestingly, the intestinal epithelium has distributed divergent biological tasks through only four differentiated cell types.

Two main lineages of differentiated cell types are discerned within the intestinal epithelium: the enterocyte or absorptive lineage and the secretory lineage. The latter lineage encompasses goblet cells, the enteroendocrine lineage, and Paneth cells. Enterocytes are abundant in the small intestine, secreting hydrolases and absorbing nutrients. Goblet cells, secreting protective mucins, increase in numbers from the duodenum (starts right after the stomach) to the colon. Enteroendocrine lineage cells secrete hormones, e.g., serotonin, substance P, or secretin [26], and these represent a small proportion (less than 1%) of all cells. Paneth cells reside only in the small intestine and are positioned at the crypt bottom. Paneth cells secrete antimicrobial agents such as cryptdins, defensins and lysozyme to control the microbial content of the intestine [27,28].

The formation of distinct compartments and different cell lineages of the intestinal epithelium is governed by a network of signaling cascades like Wnt, Notch, BMP and Hedgehog. The most prominent among them is the Wnt pathway that controls the renewal and proliferation of the IECs [1,2]. In addition, Wnt induces an anti-microbial activity by activating the expression of the MMP7/cryptidin program in specified Paneth cells [29,30]. Wnt components such as frizzled, β-catenin and TCF4 are expressed in the proliferative crypts progenitors of the intestinal epithelium. However, Wnt signaling is also responsible for tumorgenesis under abnormal activation. Mutations in the APC gene were identified as the causative basis for familial adenomatous polyposis coli (FAP), a heritable predisposition to colorectal cancer [2,12]. Taking all together, tight regulation of the Wnt signal is required to maintain gut homeostasis.

Tiny but mighty microRNAs: Their role and biogenesis

The discovery of small non-coding RNA molecules that differ from coding RNA opened a new horizon in our understanding of cellular systems complexity in the last 20 years. Special attention was given to the unearthing of the RNAi phenomenon, such as small interfering RNAs (siRNA) and microRNAs (miRNAs or miRs), which ignited the field of post-transcriptional regulation. The cellular RNAi machinery, which acts through microRNAs, may control the initiation of protein production in two ways: messenger RNA (mRNA) degradation or protein synthesis arrest. The first microRNA to be discovered was lin-4 in nematodes [31], and since then about 530 microRNAs have been annotated in humans. Recent estimations suggest the existence of 500–1000 miRNAs per genome and that a large proportion of human protein-coding genes are under the regulation of one or more miRNAs [32,33]. In short, microRNA biogenesis starts with RNA polymerase II transcription within the nucleus, as pol II long transcript containing a 7mG cap and a poly-A tail. A nuclear endonuclease Drosha, together with the RNA binding protein, Pasha compose the microprocessor

complex that cleaves the long transcript (pri-miRNA) into ~70 nucleotides stem–loop RNA known as pre-miRNA, which is then exported to the cytoplasm by Exportin-5. In the cytoplasm, Dicer a second RNase III like enzyme further processes the pre-miRNA into a small double-strand RNA (dsRNA) of about 18-27 nucleotides. This dsRNA unwinds via a helicase-like enzyme and the mature microRNA is then loaded into the RNA induced silencing complex (RISC) [34,35]. This RNP complex binds to specific mRNA transcripts and inhibits gene expression. This association depends on sequence complimentary, where the microRNA "seed" sequence is nearly matching to the sequence of the mRNA target 3' UTR. Furthermore, it was recently shown that under specific circumstances, microRNAs not only suppress but can also activate protein synthesis [36]. MicroRNAs in general seem to be tiny regulators of the cell that can rapidly switch on and off the activation of a vast array of signaling networks related to development, cell proliferation and even tumorgenesis.

The RNAi machinery: endonucleases

Endoribonuclease III (RNase III) was the first dsRNA specific endoribonuclease to be discovered in *E. coli.* In the human genome there are two RNase III like enzymes which play key roles in the RNAi machinery, Dicer and Drosha [37,38]. They regulate a wide variety of other genes by interacting with the RISC to induce cleavage of complementary mRNA or protein synthesis arrest [39]. Drosha initiates the processing of pri-miRNAs or short RNA molecules in the nucleus after their transcription. Dicer cleaves dsRNA and pre-microRNA into short siRNA of about 18-27 nucleotides long, usually with a two-base overhang on the 3' end [38,40]. Dicer contains two RNase III domains and one PAZ domain (dsRNA binding domain); the distance between these two regions of the molecule is determined by the length and angle of the connector helix and determines the size of the siRNAs it produces [41]. Dicer catalyzes the cleavage of mature microRNA and initiates formation of the RISC, whose catalytic component argonaute (Ago) is an endonuclease capable of degrading mRNA with a sequence complementary to that of the siRNA guide strand [42].

Preliminary Results

Hunting for Wnt microRNA candidates

Knowing that the Wnt pathway is tightly regulated encouraged us to investigate the role of microRNA in this system. A genomic scale bioinformatics approach was first used to find microRNAs that can be regulated by Wnt pathway. Tcf/Lef sites in the genome can implicate specific genes as targets of the Wnt pathway. Using a known data set and a TRANFAC algorithm matrix, we found the consensus sequence for Tcf/Lef transcription factors [43,44]. We then searched at the 10kb

upstream for each microRNA known at that time (360 miRs), using restricted parameters (Fig. 1A.) and found nine microRNA candidates, which may be regulated by the Wnt pathway (Table 1, left panel). Surprisingly, most of these microRNAs have Wnt related genes as predicted targets within known target prediction software [33,45-47]. The most striking unique group of microRNAs appeared within our list was the miR-103 family, which is composed of miR-103-1, miR-103-2 and miR-107 (Fig. 1B&C). The existence of three similar miRs at different locations of the genome, which still reserve Tcf/Lef sites within their assumed promoter, suggests that these miRs are important targets of the Wnt cascade. Since feedback mechanisms play a major function in all signaling cascades, we checked whether this miR family could regulate Wnt signaling components. Almost all of our predicted miRs had more than one Wnt related gene as putative targets, and Axin2 was a highly predicted candidate for the miR-103 family (Table 1, right panel and Fig 3C). In agreement with this notion, our data suggests that miR-103 family regulates the protein level of a Wnt pathway target gene, Axin2 (Fig. 4Ab). Using two different colorectal cell lines (CRCs), RKO and CaCo2, we showed that both under Drosha silencing and miR-103 over-expression (OE, Fig 4Ac), Axin2 protein levels are altered, especially under Wnt stimulation (Fig. 4A and B). These results may suggest the requirement of miR-103 in the regulation of Axin2 protein levels in order to prolong Wnt signaling activity. Furthermore, a bioinformatic work in proof of concept showed that miR-103 binds and represses the E3 ligase of β-catenin, β-TrCP1, by a 3' UTR luciferase assay [48]. It would be interesting to determine if miR-103 family controls another negative regulator of the Wnt cascade rather than Axin2, such as β-TrCP1. With this in mind, we chose to further investigate the role of microRNAs, and in more detail, the role of the miR-103 family in the Wnt pathway.

Involvement of microRNAs in the Wnt signaling.

In order to examine whether microRNAs play a role in the regulation of the Wnt pathway, we decided to globally inhibit the RNAi machinery, and by that, inhibit the formation of mature microRNAs. Choosing the best *in vitro* Wnt system is not obvious. Most colorectal cell lines harbor high levels of β-catenin due to mutation in the Wnt signaling. We chose to stimulate the Wnt ligand in the RKO colorectal cell line in which the Wnt signaling is responsive. The RKO cell line has low β-catenin levels while its phosphorylation level is considered to be fairly high. We then stimulated the RKO cell line with Wnt 3A ligand in a time course ranging from 0 to 2.5 hours. We observed changes in β-catenin phosphorylation, starting by a massive reduction after 30 minutes and then gradual increment almost to the basal level over time. The reduction in phosphorylation allowed

β-catenin to accumulate even after the β-catenin phosphorylation state was nearly resumed (Fig. 3B). We then infected the RKO cell line with a third generation lentivirus construct containing shRNA against Drosha (Fig. 2A). The silencing of Drosha resulted in an accumulation of pri-miRs and a reduction of mature miRs (Figure 2B and 3A). Under Wnt 3A induction, Drosha knockdown (KD) caused a higher accumulation of β-catenin and a profound reduction in its phosphorylation (Fig. 3B). Comparing the ratio between β-catenin level and its phosphorylated form revealed that under Drosha KD, Wnt signaling prolongs its activation (Fig. 3B). This result leds us to suspect that microRNAs may have a role in the repression of Wnt signaling under Wnt stimulation.

Generation of gut conditional and inducible Dicer knockout mouse

A massive β-catenin accumulation under Drosha knockdown led us to wonder whether we can observe an accumulation of β-catenin in colonocytes by creating a mouse model in which mature microRNAs are inhibited. Therefore, we decided to explore the role of microRNAs in the intestinal tract of adult mice. The intestine is a constantly regenerative tissue which is mainly controlled by the Wnt pathway. The major incidence of human colon cancer is attributed to abnormal activation of this pathway. Dicer-null mouse embryos arrest development at E7.5 well before the formation of the intestinal tract [49]. To investigate our hypothesis, a dicer conditional allele ($Dicer^{flox}$) mouse was generously provided by the J. Tabin's group. We then crossed this mouse to a heterozygous transgenic mouse expressing the tamoxifen-inducible Cre recombinase construct, $CreER^{T2}$, downstream to villin promoter, a specific epithelial intestine expressed gene (Fig. 5A) [50]. $CreER^{T2}$ encodes a Cre recombinase (Cre) fused to a mutant estrogen ligand-binding domain (ER^{T2}) that requires the presence of tamoxifen for activity. After tamoxifen induction, cre-mediated recombination results in the inactivation of Dicer within the IECs and the reduction of mature microRNAs (Figure 5B).

Immune deficiency and aberrant epithelial differentiation in Dicer null mouse

Upon dicer deletion we found changes in small intestine cell differentiation, mainly the reduction of mature Paneth cell formation and an accumulation of intermediate cells (this could indicate of a Paneth cell progenitor) in IECs dicer depleted mice (Fig. 5C and 6). Paneth cell differentiation is mainly associated with Wnt activation within the crypt [51]. Recently it was shown that Sox9 is an early transcription factor which is essential to Paneth cell formation [51,52]. We hypothesized that Sox9 could be regulated by our predicted specific Wnt microRNA/s (Table 2). In this hypothesis, upon Wnt activation, Sox9 protein levels accumulate and during the same time

frame, Wnt specific miR gradually accumulates and could counteract Sox9 accumulation and subsequently reduce Sox9 protein levels. This late reduction of Sox9 can promote the final maturation of Paneth cells. Interestingly, examining Sox9 mRNA levels revealed that it may be elevated by about 20% although this isn't conclusive (Data not shown). Next, we intend to check Sox9 protein levels in small intestine crypts.

Upon inactivation of dicer, a massive reduction in mature goblet cell formation (goblet depletion) is observed in the large intestine (LI). This reduction is accompanied by reduction in goblet cell markers and a strong nuclear staining of β-catenin (Fig. 7). Wnt signaling promotes the proliferation of enterocytes and inhibits the differentiation of goblet cells in the colon (Fig 7Ab&c) [1,14]. The accumulation of β-catenin in the nucleus resulted in the elevation of Wnt target genes in the colonocytes upon the following time of tamoxifen induction (Fig. 7 B&C). These results correlate with the *in-vitro* analysis of Drosha KD in CRCs (Fig. 3B). The differentiation of goblet cells is a combinatory signaling effect that include the reduction of Wnt and Notch signaling [30,53]. Goblet cells are responsible for secreting mucus, which protects the enterocytes from infectious agents, and therefore plays a role as an immunity agent in the intestinal epithelium.

The gut epithelial cells also have an immunological function and form a barrier between the outside world and the body. Thus, we examined their immunological properties and to our surprise, we found immunological defects in the gut of dicer-depleted mice. Our inspection of the colon microflora revealed a spontaneous parasite overload, in spite of the fact that our mice were kept in an SPF unit (Fig. 8A). Parasites are largely cleared by the Th2 response arm and parasitic infections may occur due to a drop in Th2 cytokines within the colon. To investigate this, we measured Th2 cytokine mRNA levels, finding a reduction of 30-50% in the major Th2 cytokines levels, compared to control mice (Fig. 8B). Based on these results, we set up an *in-vivo* model to estimate the functionality of the Th2 response in the gut. This model consist of controlled infection of *Trichuris muris*, an intestinal helminth infectious agent, which resides mainly in the cecum of T cell deficient mice[24,54]. C57B/6J mice are known to resist *T. muris*, yet Dicer-deficient C57B/6J mice are susceptible to *T. muris* infection, suggesting that in part, microRNAs are governing the immune homeostasis of the gut (Fig. 9A&B).

These results can be partially explained by a crosstalk between IECs and the innate and adaptive immune system. Indeed, several studies have demonstrated the importance of enterocyte-specific cytokines and factors such as thymic stromal lymphopoietin (TSLP), and resistin-like molecule (RELMβ) in the maintenance of gut homeostasis [20,21,24,55,56]. In *T. muris* infected dicer-

depleted IECs mice, we further observed a severely enhanced goblet cells hypoplasia (data not shown) and reduction of goblet cell effector-molecule expression, such as RELMβ, and the enterocyte cytokine TSLP (Fig. 8C&9) suggesting that changes in the microflora may be responsible in part for the abnormal differentiation of IECs.

To surmise, the immunological defect in a dicer mutant gut may be derived from at least three mechanisms: firstly, there is poor differentiation of specialized IECs that normally provide host defense, secondly, infections due to poor IEC protective function fail to trigger the correct immune response, and thirdly, failure of IECs to induce the correct immune response causes further perturbations in IEC differentiation.

Research goal

Our hypothesis is that microRNAs play a defined role upstream and downstream of the Wnt signaling pathway. We will apply different approaches to address the hypothesis, starting from bioinformatics, continuing with an *in-vitro* study and finally examining the role of microRNA in a Wnt dominant environment; the intestine of adult mice.

Our specific aims are:

1. Identify Wnt related microRNAs and their target genes.
2. Find the functionality of these microRNAs as either regulators or effectors of the Wnt signaling pathway using *in-vitro* and *in-vivo* systems.
3. Understand the role of microRNAs in gut homeostasis and particularly their effects on the different compartments of the intestine using our dicer depleted IECs mouse model.

Research plan

Identifying Wnt related microRNA and their target genes

Global microRNA expression pattern under Wnt induction may help us to understand better the complexity of microRNA regulation in the Wnt pathway. Using a miR-array of different time courses under Wnt simulation, we can identify microRNAs that are regulated by the Wnt pathway (up-regulated) and also microRNAs that constantly regulate the activation of Wnt (down-regulated) in RKO cell lines. It is hoped that this experiment will point to specific microRNAs whose expression can be later validated using RT-qPCR. After confirming the expression of miRs, using miR manipulation techniques, such as over-expression and inhibition of specific miRs, we could test

their role in Wnt signaling. First, by checking different colorectal cell lines, we can determine whether the expression of specific miRs, such as miR-103, may altar β-catenin accumulation, Wnt activation kinetics, and the expression of Wnt target genes, as shown in figure 4. Second, we aim to identify and test microRNA targets genes by bioinformatics and biochemical tools, which include luciferase assays of candidate targets, as shown in figure 4A, and the purification of polysome bodies (p-bodies) under Wnt stimulated cells with or without Drosha knockdown. P-bodies are suggested to participate in the RNAi machinery by sequestering the miRNA protected mRNA targets (for further reading see [57-60]). Purification of p-bodies could help us to detect miRNA target genes on the mRNA level. A gene expression array will be performed on purified p-bodies RNA in an effort to elucidate which miRNA target genes are affected by the activation of the Wnt pathway. Third, using SILAC (Stable isotope labeling with amino acids in cell culture) technology for mass-spectrometry under Wnt stimulation in suitable colorectal cell lines, which we are currently attempting to calibrate, we can identify miR target genes by comparing the protein levels that will alter during Wnt stimulation [61,62]. In sum, the integration of multiple approaches, from the identification of Wnt related miRs, gene expression alteration under the manipulation of specific miRs, to gene expression upon Wnt activation with or without global miR expression, will give us a better understanding of how microRNAs affect the Wnt signaling pathway.

The biological function of Wnt related microRNAs

Our preliminary results suggest that microRNAs are taking an active part in Wnt signaling regulation. We found a "Wnt" miR-103 family that elevates upon Wnt induction and controls the expression of a known Wnt target gene, Axin2, in several colorectal cell lines (Figure 4). As mentioned in the introduction, Drosha is a key component of the RNAi machinery that cleaves pri-miRNA into pre-miRNA. Using this construct, we can eliminate newly endogenous synthesis of most microRNAs, but can also introduce shRNA constructs (which resemble pre-miRNA) into cell lines and by that examine each microRNA function within the Wnt pathway.

In order to test the effects of specific miRs on the Wnt cascade, such as miR-103, we will examine its effect on β-catenin accumulation, phosphorylation and the downstream effect on target gene induction. The intestine enterocyte cells polarize upon their differentiation [56]. In our lab there is a polarized CaCo2 cell system (which are cultivated in trans-wells) to imitate as much as possible the enterocyte cells found *in-vivo*. In this system, we noticed that Axin2 protein levels are extremely low, but its mRNA levels did not change. However, when CaCo2 cells are not polarized,

Axin2 protein levels are high (Farago et al., unpublished data). Is it possible that miR-103 is important for reducing Axin2 levels upon polarization of CaCo2? Our system allows us to answer this question. Using Drosha KD, miR-103 OE and miR-103 inhibition (antagomiRs), we can check Axin2 protein levels in CaCo2 polarized cells. If indeed our assumption is correct, miR-103 keeps Axin2 levels low in order to prolong Wnt signal within these cells. It is a possibility that the role of miR-103 is to mildly prolong Wnt signaling by inhibiting negative players of the Wnt cascade. Wnt signaling may sustain its activation by choosing the most rapid and low energy control mechanism, such as microRNAs to inhibit negative regulators like Axin2 at the post-transcriptional level. This regulation is temporal, and upon continued Wnt activation, is released by shifting the balance to reduce Wnt signal programming [63-65].

The role of MicroRNA in gut homeostasis

Our preliminary results suggest that aberrant developmental changes caused by lack of mature microRNAs affect mostly the "immune" intestine epithelial cells (Fig. 6&7). The reduction of goblet cells in the colon under dicer inactivation is profound. Goblet depletion leads to changes in the normal lumen environment, which allows pathogenic microflora to accumulate (Fig. 8). Subsequently, microflora overload enhances the developmental defects that we find (Fig. 9). In order to study and overcome these issues, we designed the following experiments:

1. The creation of dicer inactivated IECs in T cell deficient mice (Nude mice). There is a possibility that our phenotype initiates by defects in the T cells response, through high levels of Th1 and low levels of Th2, leading to chronic inflammation of the bowel. A Th2 response is known to promote the differentiation of goblet cells in the colon [66]. Improper balance between Th1 and Th2 response could account for the lack of mature goblet cells in the colon. This experiment will give us a clue whether the reduction of mature microRNAs cause an abnormal immune response initially that causes aberrant IECs differentiation later on. A quicker method for creating T cell deficient mice will be to treat IECs Dicer deleted mice with cyclosporin A. Cyclosporin A is an immunosuppressant drug widely used in post-allogeneic organ transplants to reduce the patient's immune response and the risk of organ rejection. Cyclosporin A mainly inhibits the transcription of interleukin-2. It also inhibits lymphokine production and interleukin release, and therefore leads to a reduced function of effector T-cells. If we suppress the immune system and a partial rescue of our phenotype will be found, we could suggest that an immunological defect is first to appear, leading subsequently to aberrant developmental processes in the gut. Importantly, by controlling these experiments, an attention should be paid to the gut developmental effects associated with immunomodulation (i.e., in Dicer

proficient animals).

2. The parasite model of *T. muris* showed that under pathogen infection, goblet cell depletion is more severe (data not shown) and that the imbalance between Th1 and Th2 is diverted further to Th1 on the expense of Th2 (Fig. 8D). This suggests that the spontaneous infection by pathogenic microflora may play a role in gut homeostasis of dicer depleted IECs mice. In which way the microflora may contribute to gut abnormality under dicer depletion? The elimination of microflora overload in dicer deleted IECs may rescue a portion of the abnormalities in the gut. First, we will monitor differentiation processes in the gut, looking for Paneth cells in the small intestine, and goblet cell formation in the colon. Second, we will examine Th2 cytokines and goblet cell effectors, such as RELMβ and TSLP, in the small and large intestine. This experiment will help us to pin point secondary effects of Dicer depletion. If we will observe goblet cell formation in the large intestine or Paneth cell maturation in the small intestine, it will suggest that this differentiation abnormality is a secondary effect caused by the microflora burden.

3. We aim to find specific microRNAs and their target genes that can account for normal gut homeostasis. Dicer depletion in the gut results in distinct morphological changes in the large and small intestine. These changes appear to be unique to a specific compartment of the gut tissue. In the small intestine we can easily detect goblet cell formation, but not Paneth cell maturation within the crypts, while in the large intestine we observed goblet cell depletion under Dicer inactivation. These results suggest that each gut compartment may have different signaling networks, resulting in specific microRNA expression patterns. A comparison of gene expression and microRNA expression of the same sub-compartment of the gut will give us a better understanding of which microRNAs govern this compartment. This may lead to the discovery of these miRs target genes that could account for normal differentiation of specific IEC. To answer these questions, we will isolate LI crypts, SI crypts and SI villi following two weeks of dicer depletion vs. control. This time point is where we can first observe morphological changes under dicer depletion, while some microRNAs may still not be inhibited. RNA from these samples will be subjected to miR-array in collaboration with Rosetta Genomics Inc. RNA from the same compartment following one month of dicer depletion and control, were already subjected to an expression array. Mild and highly up-regulated and down-regulated genes extracted for this analysis will be compared to down-regulated miRs in the same compartment. This cross-analysis holds a good chance of implicating target genes to a specific microRNA. Further validation of these targets will be done *in vitro* using colorectal cell lines.

References

1. Clarke, A.R. Wnt signalling in the mouse intestine. *Oncogene* **25**, 7512-21 (2006).
2. Clevers, H. Wnt/beta-catenin signaling in development and disease. *Cell* **127**, 469-80 (2006).
3. Taketo, M.M. Wnt signaling and gastrointestinal tumorigenesis in mouse models. *Oncogene* **25**, 7522-30 (2006).
4. Schweizer, L. & Varmus, H. Wnt/Wingless signaling through beta-catenin requires the function of both LRP/Arrow and frizzled classes of receptors. *BMC Cell Biol* **4**, 4 (2003).
5. Amit, S. et al. Axin-mediated CKI phosphorylation of beta-catenin at Ser 45: a molecular switch for the Wnt pathway. *Genes Dev* **16**, 1066-76 (2002).
6. Barker, N., Morin, P.J. & Clevers, H. The Yin-Yang of TCF/beta-catenin signaling. *Adv Cancer Res* **77**, 1-24 (2000).
7. Korinek, V. et al. Two members of the Tcf family implicated in Wnt/beta-catenin signaling during embryogenesis in the mouse. *Mol Cell Biol* **18**, 1248-56 (1998).
8. Brantjes, H., Roose, J., van De Wetering, M. & Clevers, H. All Tcf HMG box transcription factors interact with Groucho-related co-repressors. *Nucleic Acids Res* **29**, 1410-9 (2001).
9. Jho, E.H. et al. Wnt/beta-catenin/Tcf signaling induces the transcription of Axin2, a negative regulator of the signaling pathway. *Mol Cell Biol* **22**, 1172-83 (2002).
10. Lustig, B. et al. Negative feedback loop of Wnt signaling through upregulation of conductin/axin2 in colorectal and liver tumors. *Mol Cell Biol* **22**, 1184-93 (2002).
11. Silver, S.J., Hagen, J.W., Okamura, K., Perrimon, N. & Lai, E.C. Functional screening identifies miR-315 as a potent activator of Wingless signaling. *Proc Natl Acad Sci U S A* **104**, 18151-6 (2007).
12. Polakis, P. The many ways of Wnt in cancer. *Curr Opin Genet Dev* **17**, 45-51 (2007).
13. Teller, I.C. & Beaulieu, J.F. Interactions between laminin and epithelial cells in intestinal health and disease. *Expert Rev Mol Med* **3**, 1-18 (2001).
14. Sancho, E., Batlle, E. & Clevers, H. Signaling pathways in intestinal development and cancer. *Annu Rev Cell Dev Biol* **20**, 695-723 (2004).
15. Heath, J.P. Epithelial cell migration in the intestine. *Cell Biol Int* **20**, 139-46 (1996).
16. Potten, C.S. Stem cells in gastrointestinal epithelium: numbers, characteristics and death. *Philos Trans R Soc Lond B Biol Sci* **353**, 821-30 (1998).
17. Barker, N. et al. Identification of stem cells in small intestine and colon by marker gene Lgr5. *Nature* **449**, 1003-7 (2007).
18. Booth, C. & Potten, C.S. Gut instincts: thoughts on intestinal epithelial stem cells. *J Clin Invest* **105**, 1493-9 (2000).
19. Dahan, S. et al. Epithelial: lamina propria lymphocyte interactions promote epithelial cell differentiation. *Gastroenterology* **134**, 192-203 (2008).
20. Dahan, S., Roth-Walter, F., Arnaboldi, P., Agarwal, S. & Mayer, L. Epithelia: lymphocyte interactions in the gut. *Immunol Rev* **215**, 243-53 (2007).
21. Hogan, S.P. et al. Resistin-like molecule beta regulates innate colonic function: barrier integrity and inflammation susceptibility. *J Allergy Clin Immunol* **118**, 257-68 (2006).
22. Montufar-Solis, D., Garza, T. & Klein, J.R. T-cell activation in the intestinal mucosa. *Immunol Rev* **215**, 189-201 (2007).

23. Wang, M.L. et al. Regulation of RELM/FIZZ isoform expression by Cdx2 in response to innate and adaptive immune stimulation in the intestine. *Am J Physiol Gastrointest Liver Physiol* **288**, G1074-83 (2005).
24. Zaph, C. et al. Epithelial-cell-intrinsic IKK-beta expression regulates intestinal immune homeostasis. *Nature* **446**, 552-6 (2007).
25. Shao, L., Kamalu, O. & Mayer, L. Non-classical MHC class I molecules on intestinal epithelial cells: mediators of mucosal crosstalk. *Immunol Rev* **206**, 160-76 (2005).
26. Hocker, M. & Wiedenmann, B. Molecular mechanisms of enteroendocrine differentiation. *Ann N Y Acad Sci* **859**, 160-74 (1998).
27. Ayabe, T. et al. Secretion of microbicidal alpha-defensins by intestinal Paneth cells in response to bacteria. *Nat Immunol* **1**, 113-8 (2000).
28. Jemal, A., Thomas, A., Murray, T. & Thun, M. Cancer statistics, 2002. *CA Cancer J Clin* **52**, 23-47 (2002).
29. Rath, T. et al. Enhanced expression of MMP-7 and MMP-13 in inflammatory bowel disease: a precancerous potential? *Inflamm Bowel Dis* **12**, 1025-35 (2006).
30. van Es, J.H. et al. Notch/gamma-secretase inhibition turns proliferative cells in intestinal crypts and adenomas into goblet cells. *Nature* **435**, 959-63 (2005).
31. Lee, R.C., Feinbaum, R.L. & Ambros, V. The C. elegans heterochronic gene lin-4 encodes small RNAs with antisense complementarity to lin-14. *Cell* **75**, 843-54 (1993).
32. Aravin, A. & Tuschl, T. Identification and characterization of small RNAs involved in RNA silencing. *FEBS Lett* **579**, 5830-40 (2005).
33. Lewis, B.P., Burge, C.B. & Bartel, D.P. Conserved seed pairing, often flanked by adenosines, indicates that thousands of human genes are microRNA targets. *Cell* **120**, 15-20 (2005).
34. Khvorova, A., Reynolds, A. & Jayasena, S.D. Functional siRNAs and miRNAs exhibit strand bias. *Cell* **115**, 209-16 (2003).
35. Schwarz, D.S. et al. Asymmetry in the assembly of the RNAi enzyme complex. *Cell* **115**, 199-208 (2003).
36. Vasudevan, S., Tong, Y. & Steitz, J.A. Switching from repression to activation: microRNAs can up-regulate translation. *Science* **318**, 1931-4 (2007).
37. Tijsterman, M. & Plasterk, R.H. Dicers at RISC; the mechanism of RNAi. *Cell* **117**, 1-3 (2004).
38. Zhang, H., Kolb, F.A., Jaskiewicz, L., Westhof, E. & Filipowicz, W. Single processing center models for human Dicer and bacterial RNase III. *Cell* **118**, 57-68 (2004).
39. Lee, Y. et al. The nuclear RNase III Drosha initiates microRNA processing. *Nature* **425**, 415-9 (2003).
40. Hutvagner, G. et al. A cellular function for the RNA-interference enzyme Dicer in the maturation of the let-7 small temporal RNA. *Science* **293**, 834-8 (2001).
41. Macrae, I.J. et al. Structural basis for double-stranded RNA processing by Dicer. *Science* **311**, 195-8 (2006).
42. Meister, G. et al. Human Argonaute2 mediates RNA cleavage targeted by miRNAs and siRNAs. *Mol Cell* **15**, 185-97 (2004).
43. Matys, V. et al. TRANSFAC: transcriptional regulation, from patterns to profiles. *Nucleic Acids Res* **31**, 374-8 (2003).
44. Matys, V. et al. TRANSFAC and its module TRANSCompel: transcriptional gene regulation in eukaryotes. *Nucleic Acids Res* **34**, D108-10 (2006).
45. Betel, D., Wilson, M., Gabow, A., Marks, D.S. & Sander, C. The microRNA.org resource: targets and expression. *Nucleic Acids Res* **36**, D149-53 (2008).

46. Hsu, P.W. et al. miRNAMap: genomic maps of microRNA genes and their target genes in mammalian genomes. *Nucleic Acids Res* **34**, D135-9 (2006).
47. John, B. et al. Human MicroRNA targets. *PLoS Biol* **2**, e363 (2004).
48. Kiriakidou, M. et al. A combined computational-experimental approach predicts human microRNA targets. *Genes Dev* **18**, 1165-78 (2004).
49. Bernstein, E. et al. Dicer is essential for mouse development. *Nat Genet* **35**, 215-7 (2003).
50. el Marjou, F. et al. Tissue-specific and inducible Cre-mediated recombination in the gut epithelium. *Genesis* **39**, 186-93 (2004).
51. Bastide, P. et al. Sox9 regulates cell proliferation and is required for Paneth cell differentiation in the intestinal epithelium. *J Cell Biol* **178**, 635-48 (2007).
52. Mori-Akiyama, Y. et al. SOX9 is required for the differentiation of paneth cells in the intestinal epithelium. *Gastroenterology* **133**, 539-46 (2007).
53. Leow, C.C., Polakis, P. & Gao, W.Q. A role for Hath1, a bHLH transcription factor, in colon adenocarcinoma. *Ann N Y Acad Sci* **1059**, 174-83 (2005).
54. Bancroft, A.J., Artis, D., Donaldson, D.D., Sypek, J.P. & Grencis, R.K. Gastrointestinal nematode expulsion in IL-4 knockout mice is IL-13 dependent. *Eur J Immunol* **30**, 2083-91 (2000).
55. Ben-Neriah, Y. & Schmidt-Supprian, M. Epithelial NF-kappaB maintains host gut microflora homeostasis. *Nat Immunol* **8**, 479-81 (2007).
56. Lee, J. et al. Maintenance of colonic homeostasis by distinctive apical TLR9 signalling in intestinal epithelial cells. *Nat Cell Biol* **8**, 1327-36 (2006).
57. Chan, S.P. & Slack, F.J. microRNA-mediated silencing inside P-bodies. *RNA Biol* **3**, 97-100 (2006).
58. Liu, J. et al. A role for the P-body component GW182 in microRNA function. *Nat Cell Biol* **7**, 1261-6 (2005).
59. Liu, J., Valencia-Sanchez, M.A., Hannon, G.J. & Parker, R. MicroRNA-dependent localization of targeted mRNAs to mammalian P-bodies. *Nat Cell Biol* **7**, 719-23 (2005).
60. Rehwinkel, J., Behm-Ansmant, I., Gatfield, D. & Izaurralde, E. A crucial role for GW182 and the DCP1:DCP2 decapping complex in miRNA-mediated gene silencing. *Rna* **11**, 1640-7 (2005).
61. Ong, S.E. et al. Stable isotope labeling by amino acids in cell culture, SILAC, as a simple and accurate approach to expression proteomics. *Mol Cell Proteomics* **1**, 376-86 (2002).
62. Ong, S.E., Foster, L.J. & Mann, M. Mass spectrometric-based approaches in quantitative proteomics. *Methods* **29**, 124-30 (2003).
63. Mangan, S. & Alon, U. Structure and function of the feed-forward loop network motif. *Proc Natl Acad Sci U S A* **100**, 11980-5 (2003).
64. Mangan, S., Itzkovitz, S., Zaslaver, A. & Alon, U. The incoherent feed-forward loop accelerates the response-time of the gal system of Escherichia coli. *J Mol Biol* **356**, 1073-81 (2006).
65. Yeger-Lotem, E. et al. Network motifs in integrated cellular networks of transcription-regulation and protein-protein interaction. *Proc Natl Acad Sci U S A* **101**, 5934-9 (2004).
66. Dabbagh, K. et al. IL-4 induces mucin gene expression and goblet cell metaplasia in vitro and in vivo. *J Immunol* **162**, 6233-7 (1999).

Supplementary results

Figure 1

A. TCF-4 matrix: S C T T T G A W W = A/T

LEF-1 matrix: W T C A A A G S = C/G

Conservation > 80%

Cluster ≥ 3 per 100bp

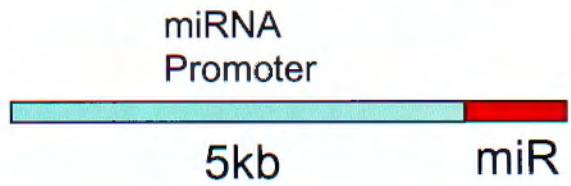

B.

Mature miRNAs

hsa-miR-103-1 AGCAGCAUUGUACAGGGCUAUGA

hsa-miR-103-2 AGCAGCAUUGUACAGGGCUAUGA

hsa-miR-107 AGCAGCAUUGUACAGGGCUAUCA

C.

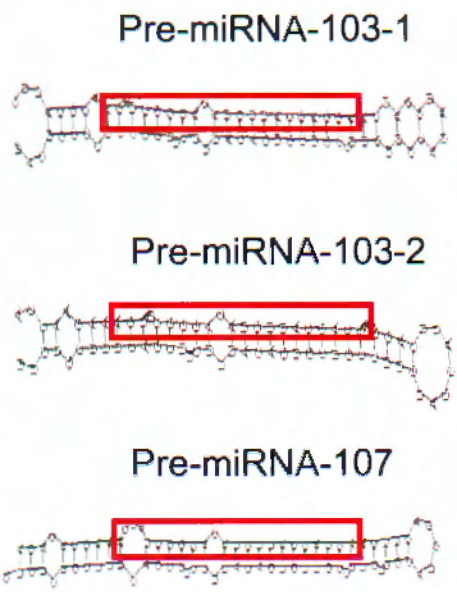

Figure 2

A.

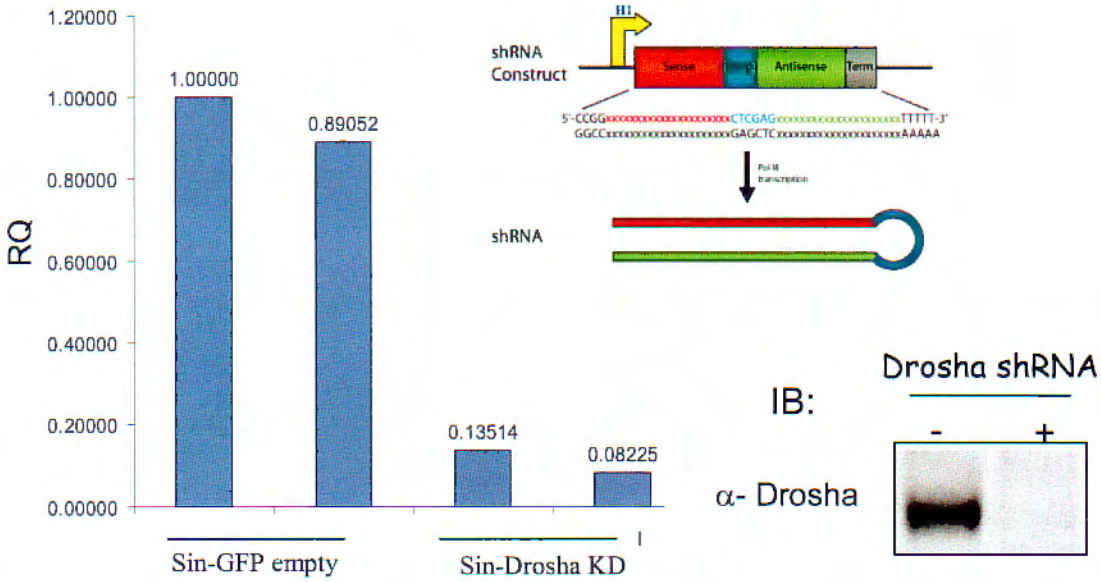
1.20000
1.00000
0.80000
0.60000
0.40000
0.20000
0.00000
RQ
1.00000
0.89052
0.13514
0.08225
Sin-GFP empty
Sin-Drosha KD
H1
shRNA Construct
Sense
Antisense
Term
shRNA
IB:
Drosha shRNA
-
+
α- Drosha

B.

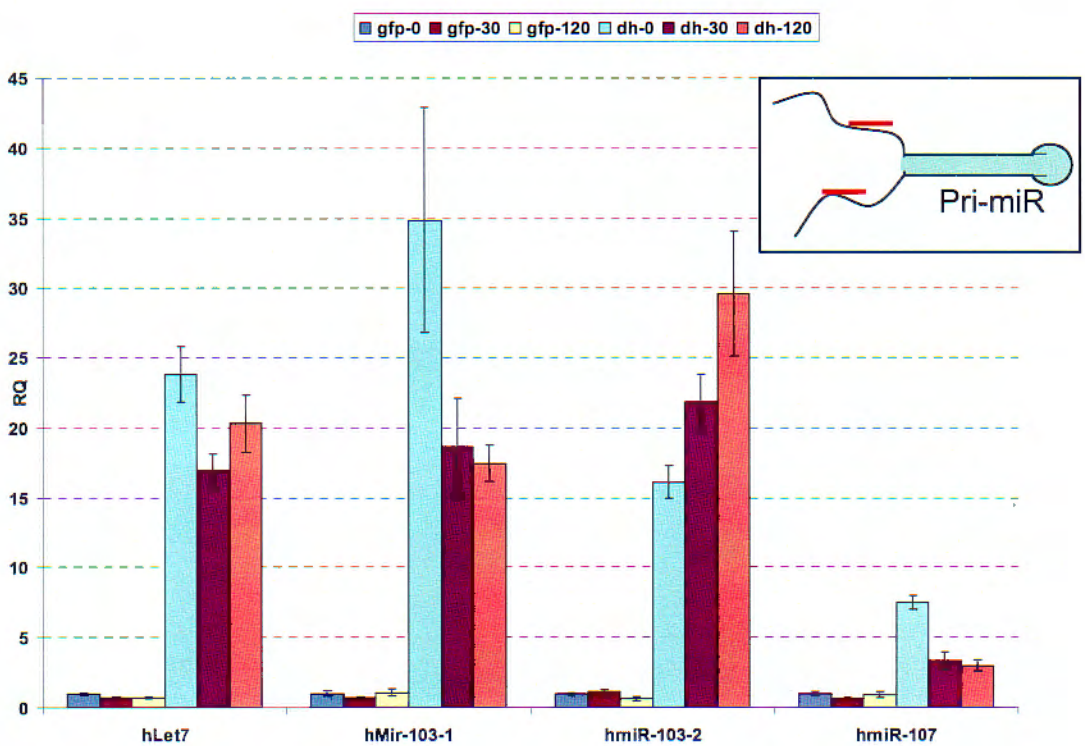
gfp-0
gfp-30
gfp-120
dh-0
dh-30
dh-120
45
40
35
30
25
20
15
10
5
0
RQ
Pri-miR
hLet7
hMir-103-1
hmiR-103-2
hmiR-107

Figure 3

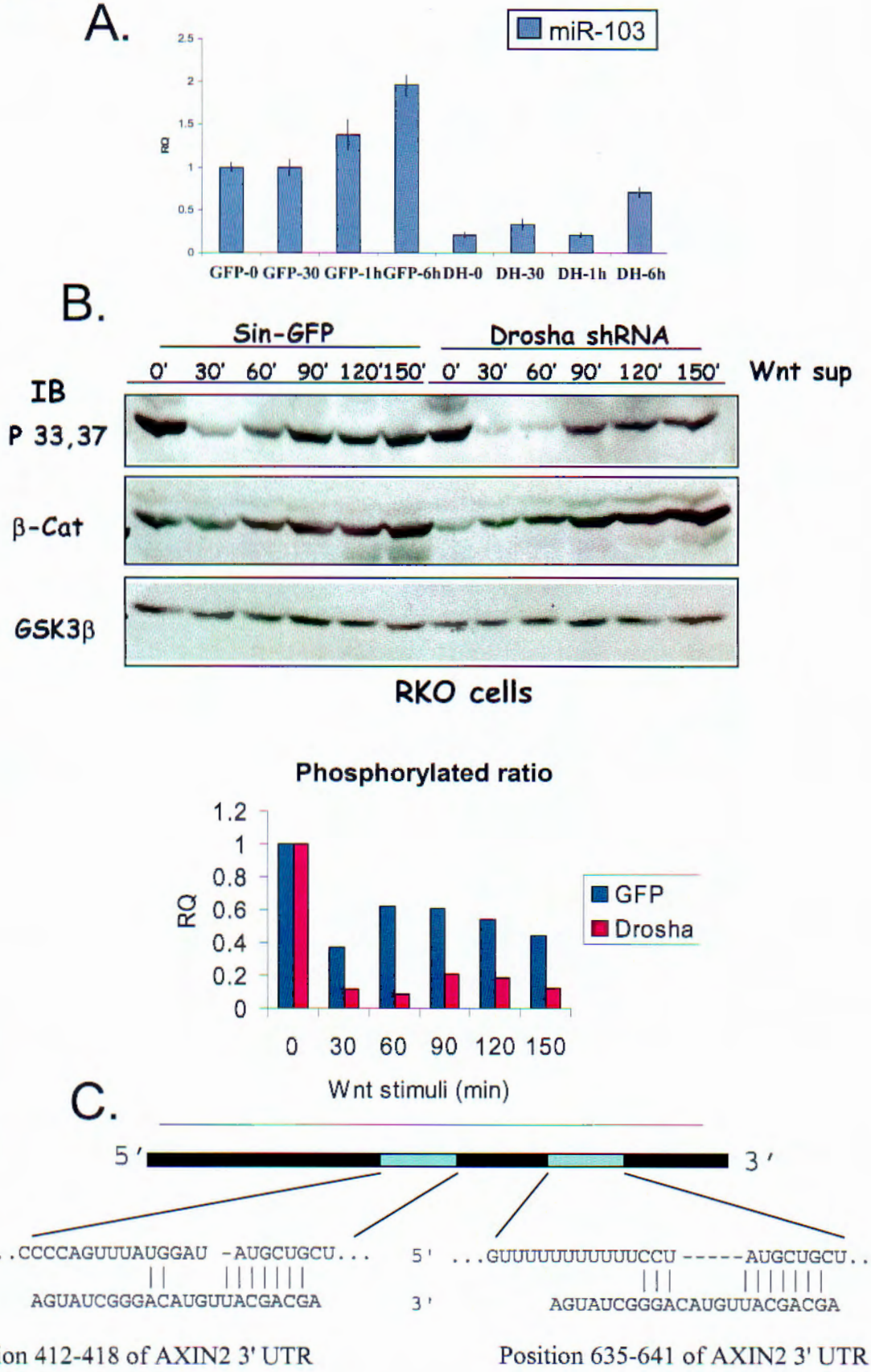

Position 412-418 of AXIN2 3' UTR

Position 635-641 of AXIN2 3' UTR

Figure 4

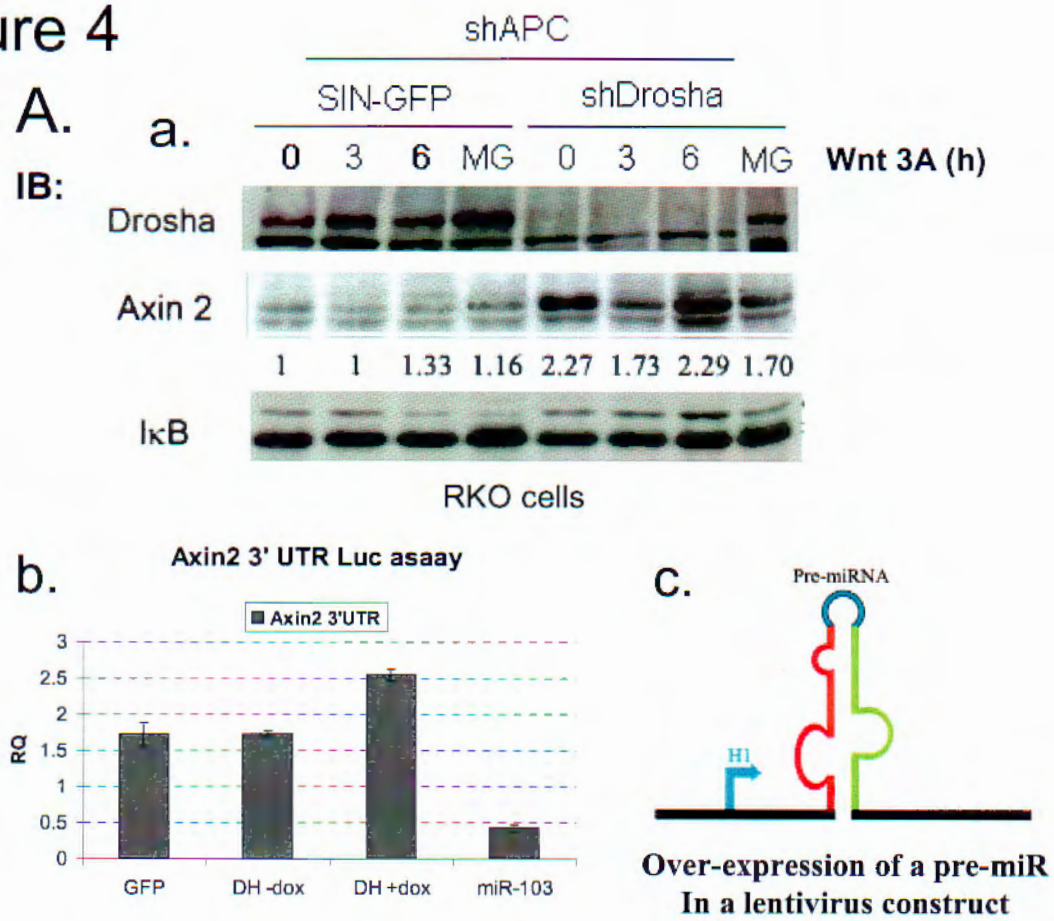
A.
a.
shAPC
SIN-GFP
shDrosha
0 3 6 MG 0 3 6 MG
Wnt 3A (h)
IB:
Drosha
Axin 2
1 1 1.33 1.16 2.27 1.73 2.29 1.70
IκB
RKO cells
b.
Axin2 3' UTR Luc asaay
Axin2 3'UTR
RQ
3
2.5
2
1.5
1
0.5
0
GFP
DH -dox
DH +dox
miR-103
c.
Pre-miRNA
H1
Over-expression of a pre-miR
In a lentivirus construct

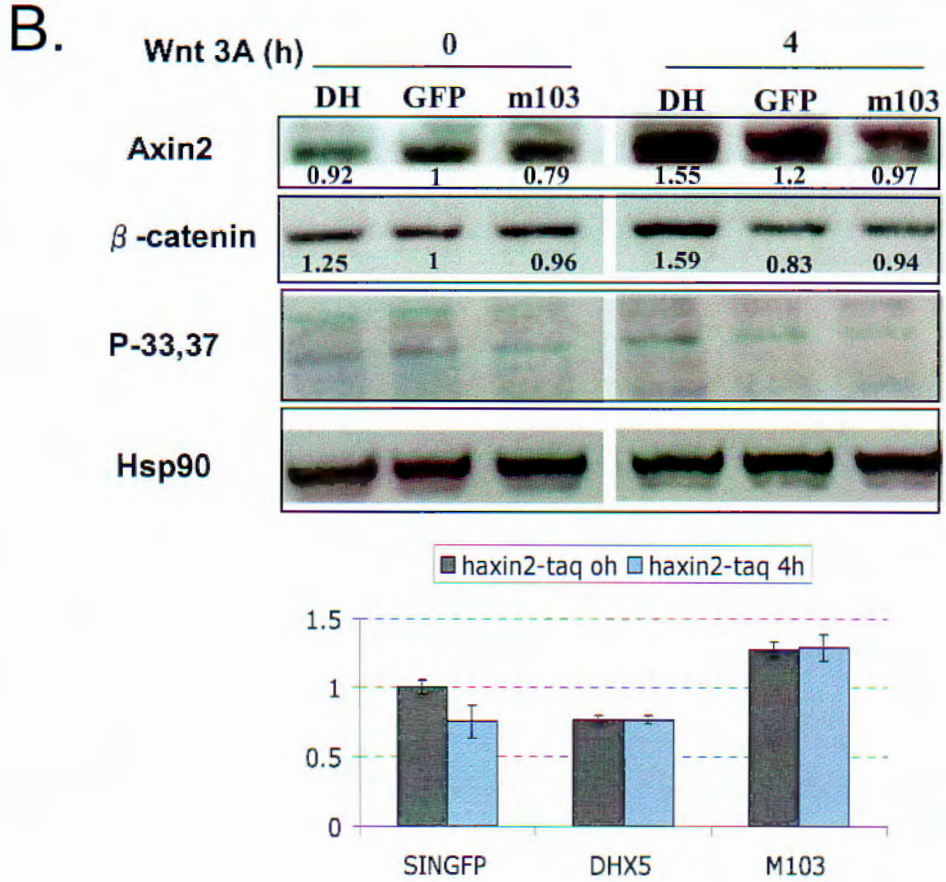
B.
Wnt 3A (h)
0
4
DH GFP m103 DH GFP m103
Axin2
0.92 1 0.79 1.55 1.2 0.97
β -catenin
1.25 1 0.96 1.59 0.83 0.94
P-33,37
Hsp90
haxin2-taq oh
haxin2-taq 4h
1.5
1
0.5
0
SINGFP
DHX5
M103

Figure 5

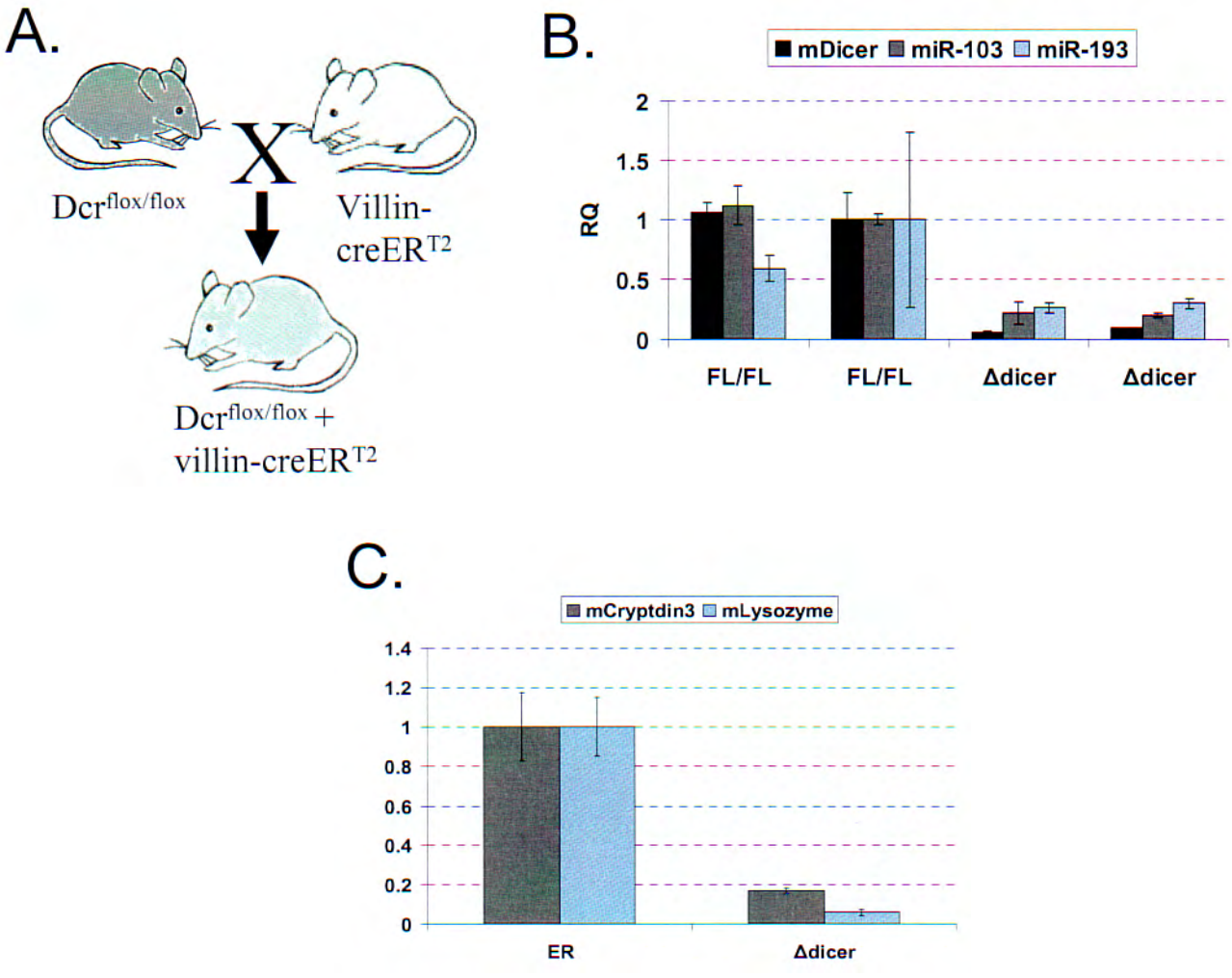
A.
Dcr^flox/flox
X
Villin-creER^T2
Dcr^flox/flox + villin-creER^T2
B.
mDicer
miR-103
miR-193
RQ
2
1.5
1
0.5
0
FL/FL
FL/FL
Δdicer
Δdicer
C.
mCryptdin3
mLysozyme
1.4
1.2
1
0.8
0.6
0.4
0.2
0
ER
Δdicer

Figure 6

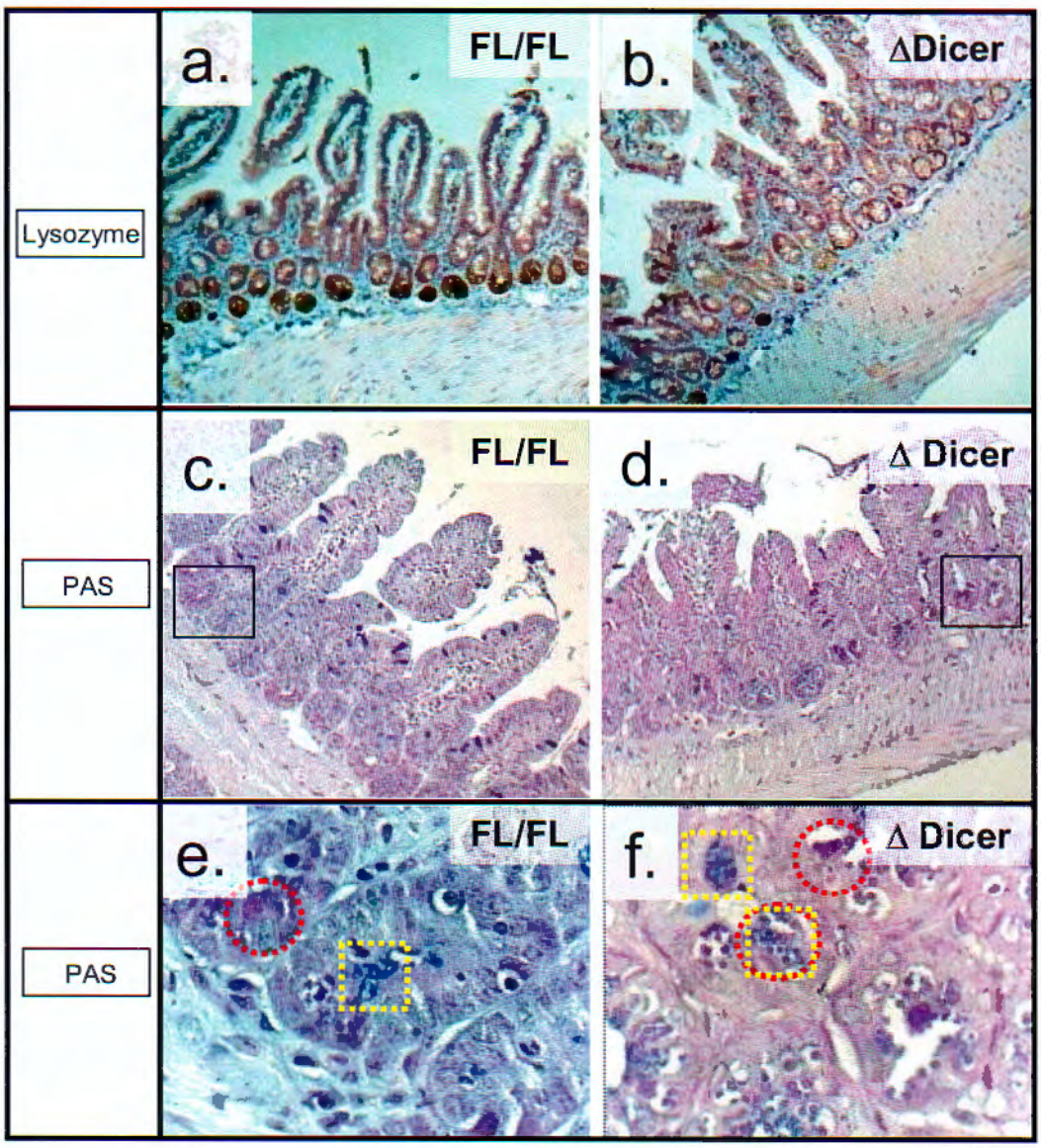
Lysozyme
a.
FL/FL
b.
ΔDicer
PAS
c.
FL/FL
d.
Δ Dicer
PAS
e.
FL/FL
f.
Δ Dicer

Figure 7

A.

a,

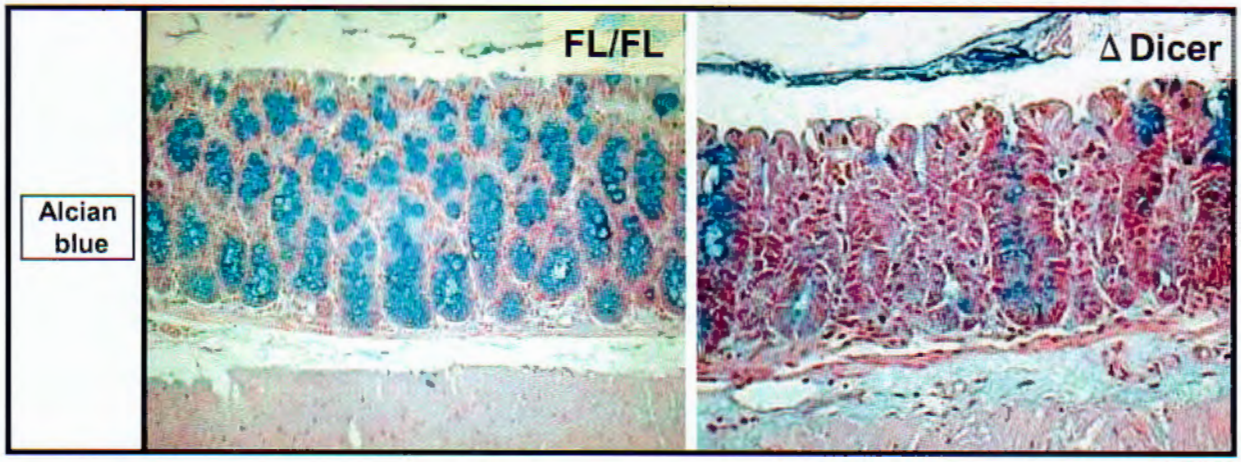

b,

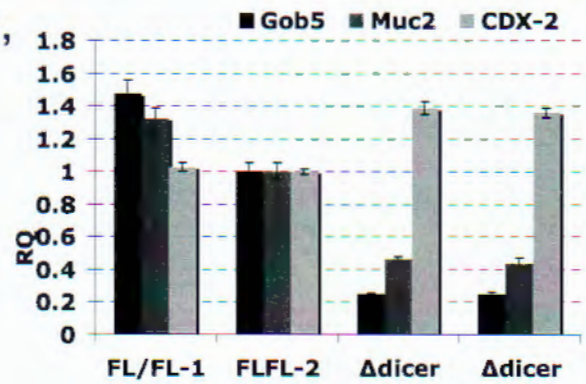

c,

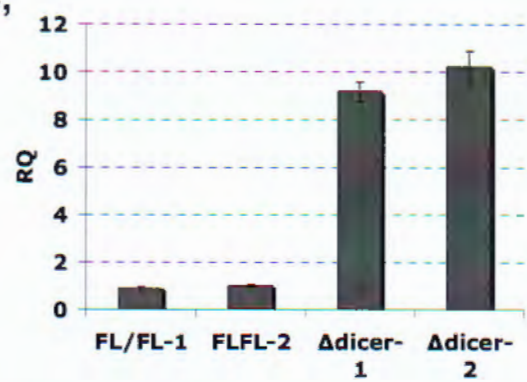

B.

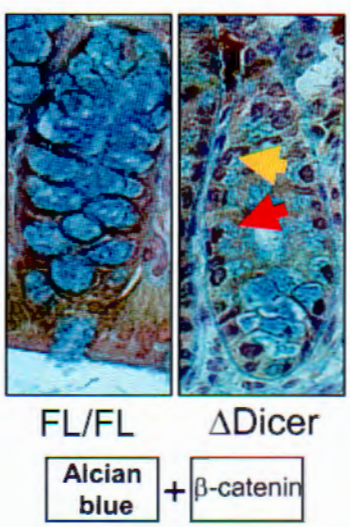

C.

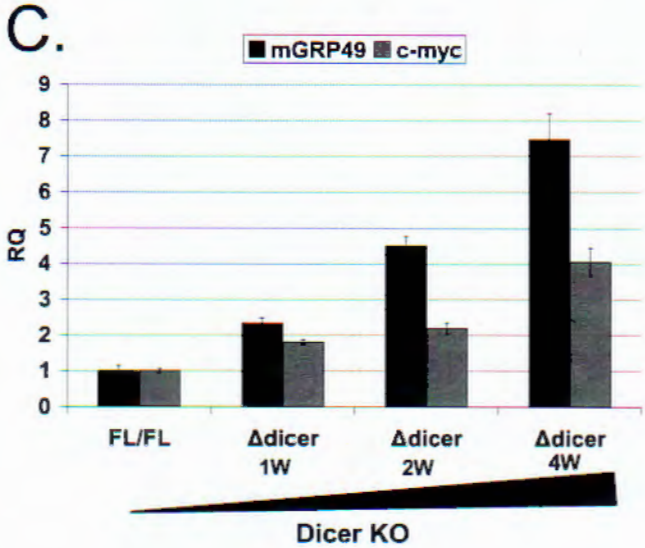

Figure 8

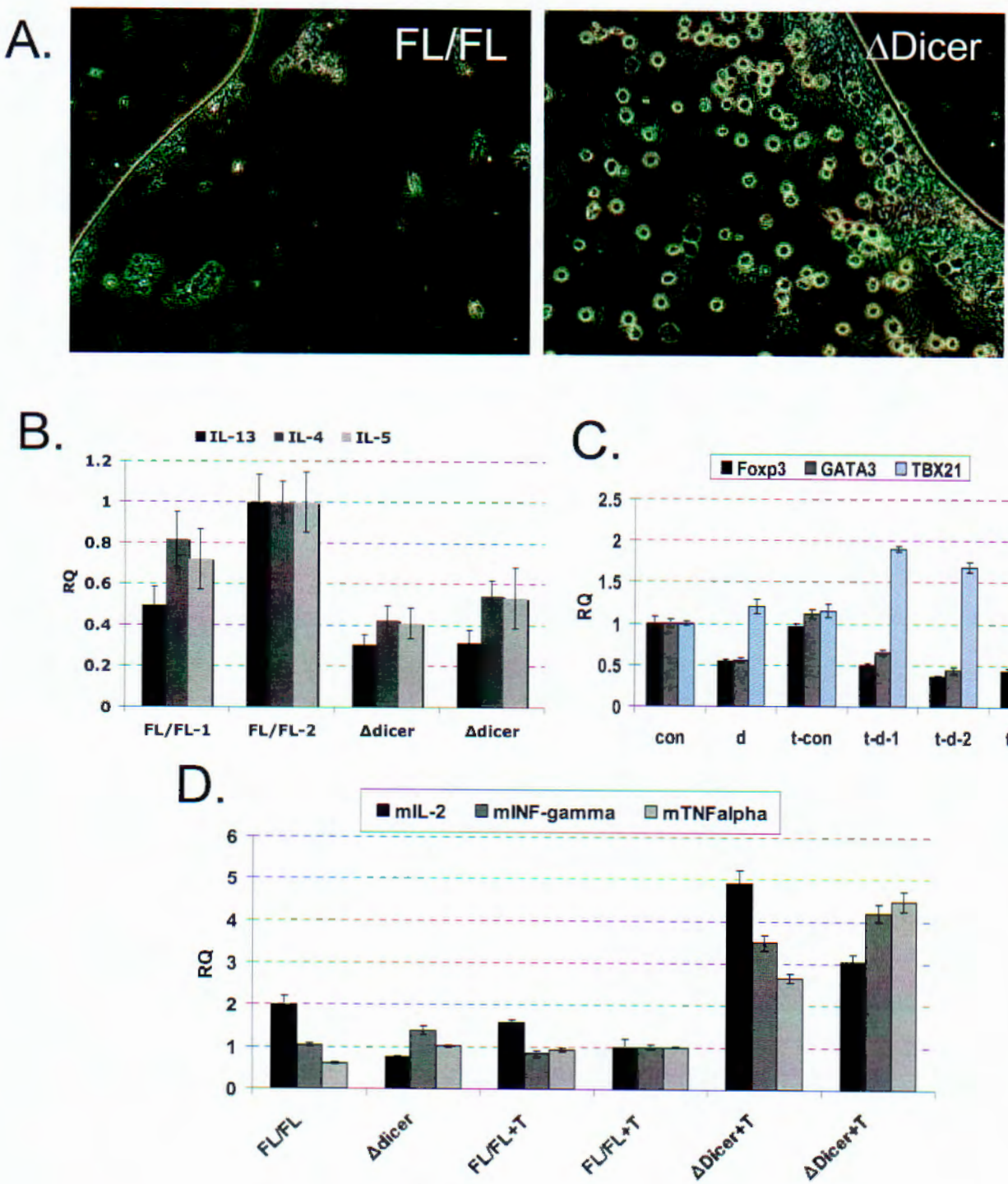
A.
FL/FL
ΔDicer
B.
IL-13
IL-4
IL-5
RQ
1.2
1
0.8
0.6
0.4
0.2
0
FL/FL-1
FL/FL-2
Δdicer
Δdicer
C.
Foxp3
GATA3
TBX21
RQ
2.5
2
1.5
1
0.5
0
con
d
t-con
t-d-1
t-d-2
t-d-3
D.
mIL-2
mINF-gamma
mTNFalpha
RQ
6
5
4
3
2
1
0
FL/FL
Δdicer
FL/FL+T
FL/FL+T
ΔDicer+T
ΔDicer+T

Figure 9

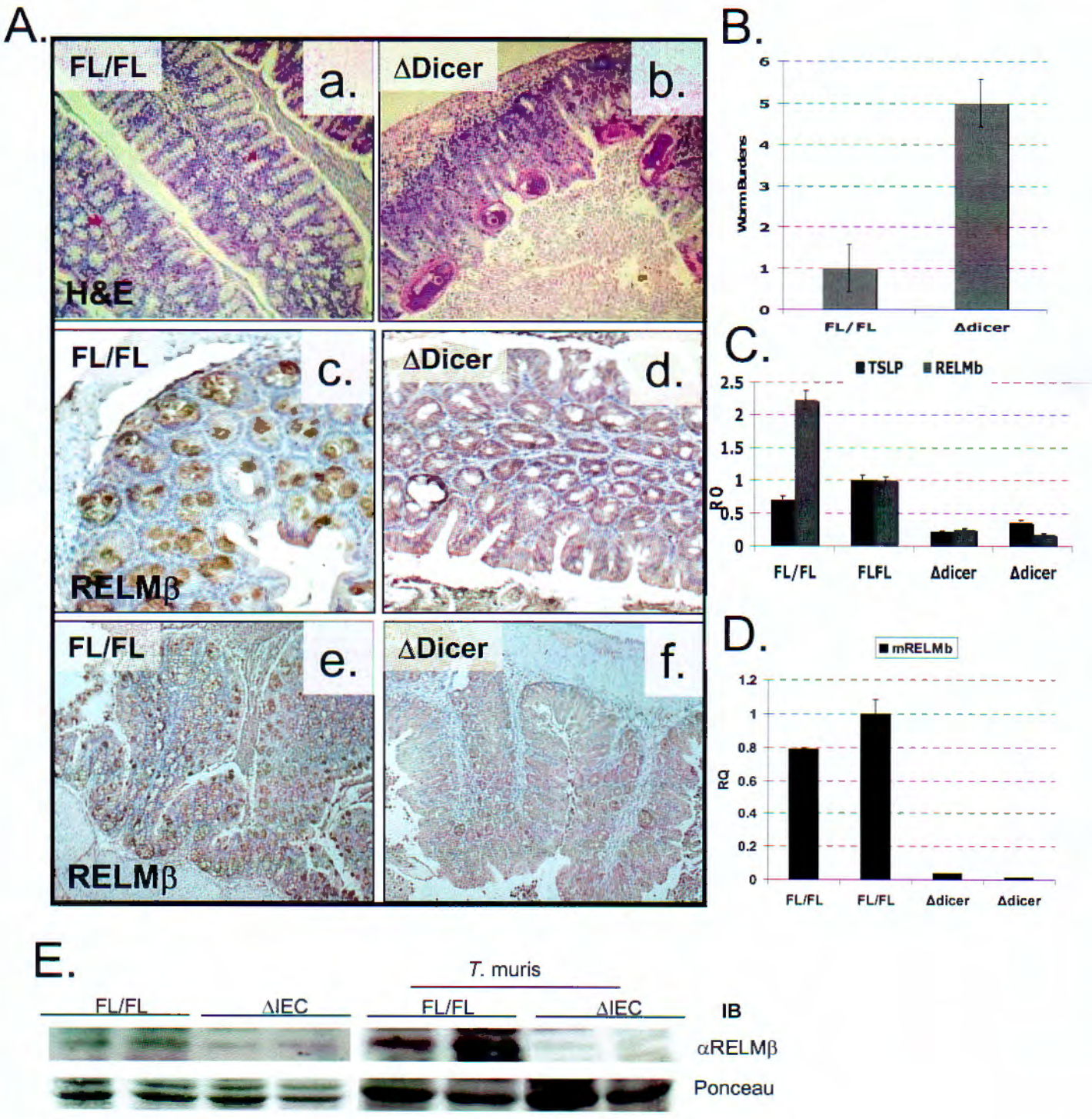
A.
FL/FL
a.
ΔDicer
b.
H&E
FL/FL
c.
ΔDicer
d.
RELMβ
FL/FL
e.
ΔDicer
f.
RELMβ
B.
WormBurders
0
1
2
3
4
5
6
FL/FL
Δdicer
C.
TSLP
RELMb
RQ
0
0.5
1
1.5
2
2.5
FL/FL
FLFL
Δdicer
Δdicer
D.
mRELMb
RQ
0
0.2
0.4
0.6
0.8
1
1.2
FL/FL
FL/FL
Δdicer
Δdicer

E.
T. muris
FL/FL
ΔIEC
FL/FL
ΔIEC
IB
αRELMβ
Ponceau

Table 1

Wnt related miRs and their putative Wnt target genes

Tcf/Lef-binding values				Target prediction software		
Gene ID	True	Max Cluster	E-value	Target Scan	Miranda	PicTar
has-Axin2	11	6	1.15e-19	control	control	control
hsa-mir-30c-1	17	6	1.001e-43	APC1,Sox9	-	PP2A
hsa-mir-30e	9	3	1.17e-22	Sox9, Sox4	APC, Mitf, PP2A	Sox9, Sox4
hsa-mir-193a	6	5	9.27e-15	PP2A	APC2, β-TrCP1, DVL1, DVL3	PP2A
hsa-mir-213	6	6	9.27e-15	-	-	-
hsa-mir-384	6	3	9.27e-15	-	-	-
hsa-mir-103-2	5	3	3.95e-12	Axin2, β-TrCP1, β-TrCP2, DVL1	Axin2, β-TrCP1, β-TrCP2,Wnt3A ,DVL1	Axin2, β-TrCP1, β-TrCP2
hsa-mir-103-1	5	4	3.95e-12	Axin2, β-TrCP1, β-TrCP2,DVL1	Axin2, β-TrCP1, β-TrCP2,Wnt3A ,DVL1	Axin2, β-TrCP1, β-TrCP2
hsa-mir-107	5	3	3.95e-12	Axin2, β-TrCP1, β-TrCP2, DVL1	Axin2, β-TrCP1, β-TrCP2,DVL1, Wnt3A	Axin2, β-TrCP1, β-TrCP2
hsa-mir-26b	4	3	1.67e-09	APC1,Lef1, Mitf	APC1, Wnt5A	GSK3 β, Lef1,

Table 2

microRNAs	predicted consequential pairing of target region (top) and miRNA (bottom)	seed match	context score percentile
Position 2111-2118 of SOX9 3' UTR mmu-miR-30b	5' ...UUUUUUGUAUAUUAUUGUUUACA... 3' UCGACUCACAUCCU---ACAAAUGU	8mer	100
Position 2111-2118 of SOX9 3' UTR mmu-miR-30e	5' ...UUUUUUGUAUAUUAUUGUUUACA... 3' UCGACUCACAUCCU---ACAAAUGU	8mer	100
Position 2111-2118 of SOX9 3' UTR mmu-miR-30d	5' ...UUUUUUGUAUAUUAUUGUUUACA... 3' UCGACUCACAUCCU---ACAAAUGU	8mer	100
Position 2111-2118 of SOX9 3' UTR mmu-miR-30c	5' ...UUUUUUGUAUAUUAUUGUUUACA... 3' UCGACUCACAUCCU---ACAAAUGU	8mer	100
Position 2111-2118 of SOX9 3' UTR mmu-miR-30a-5p	5' ...UUUUUUGUAUAUUAUUGUUUACA... 3' UCGACUCACAUCCU---ACAAAUGU	8mer	100

Figure Legends

Figure 1- Bioinformatic identification of putative Wnt regulated microRNAs
A. Tcf/Lef matrix was used to identify putative Tcf/Lef binding sites in the human genome, including in the promoters of known Wnt target genes. Under restriction parameters, such as more than 80% evolutionary conservation among 8 different vertebrates and 3 or more clusters of Tcf/Lef sites within 100bp, we searched for Tcf/Lef sites in all known microRNA "promoters"- 5Kb upstream of the mature microRNA sequence.
B. miR-103 family, which includes miR-103-1, miR-103-2 and miR-107 mature form, is illustrated. The only difference between the mature miR sequences found is marked in red.
C. miR-103 family pre-miR stem-loop. Mature miR sequences are illustrated inside the red squares.

Figure 2- Drosha knockdown and its effect on miRNA biogenesis
A. Constructing Drosha knockdown was performed by the insertion of Drosha shRNA into self-inactivated (SIN) 18 lentivirus construct containing the H1 promoter, as illustrated. RNA was extracted from the RKO cell line under Drosha knockdown. RT-qPCR was performed using specific primers and a reduction of more than 90% in Drosha mRNA levels was observed after 6 days. The experiment was conducted in biological duplicates. Protein levels of Drosha were tested by Western blot and its elimination was evident under Drosha knock-down.
B. RNA was extracted from RKO cell line under Drosha knockdown and control sinGFP, and a time course of Wnt 3A stimulation for 0, 30 and 120 minutes. Pri-miR levels of Let-7, miR-103-1, miR-103-2, and miR-107 were tested using specific primers in RT-qPCR. Under 6 days of Drosha KD all pri-miR levels were elevated, suggesting a blockage in Pri-miR processing, as might be expected in the absence of Drosha.

Figure 3- Drosha KD effects on the Wnt signaling pathway
A. miR-103 is regulated by Wnt. RNA was extracted from 6 days Drosha KD and sin-GFP (control) of RKO colorectal cells in a time course of Wnt 3A stimulation (0, 0.5, 3 and 6 hours). Elevation of mature miR-103 upon Wnt induction was measured using RT-qPCR. A reduction in mature miR levels was observed under Drosha KD, demonstrating the failure of miR biogenesis; furthermore Wnt induces synthesis of mature miR-103.
B. Drosha KD affects Wnt signaling dynamics as tested in a time course of Wnt induction (0, 30, 60, 90, 120 and 150 minutes). Western blot analysis indicates that the level of β-catenin is gradually elevated, and its phosphorylation is reduced by Wnt 3A stimulation under normal conditions (sin-GFP). β-catenin protein levels are found to be higher and its phosphorylation decreased under Wnt 3A stimulation in the absence of Drosha (Drosha KD). GSK3β protein levels are shown as a control for equal loading. The ratio of phosphorylated/ non-phosphorylated β-catenin is plotted. The control is GFP and Drosha KD is labeled as Drosha.
C. Axin2 3'UTR scheme with two predicted miR-103 family binding sites. 3' UTR of Axin2 and the predicted sites are shown in black and light blue, respectively. Magnification and miR-103 association to these sites are shown (Data taken from TargetScan 4).

Figure 4- Axin2 levels are regulated by microRNAs and miR-103 family controls the protein level of Axin2 in colorectal cell lines.
A. a, Western blot of APC KD RKO cells under a Wnt 3A stimulation (0, 3 and 6 hours) and the proteasome inhibitor MG132 (MG). Under APC KD, β-catenin levels and transcription of Wnt target genes are elevated. Drosha protein levels are reduced under the silencing of Drosha (upper panel). Axin2 protein levels are elevated under Drosha KD (mid panel). Axin2 protein levels of each lane were determined by using a densitometer. IκB protein levels (lower panel) were used as a loading control. **b,** Axin2 3'UTR luciferase assay in RKO cells. Axin2 3'UTR fraction which

contains 2 recognition sites of miR-103 family (~500bp) was fused to a luciferase (in pGL3-control vector) and transfected to RKO cells with inducible Drosha KD (DH +/- dox), miR-103 over-expression (miR-103) and control (sin-GFP). The levels of luciferase were plotted and relative quantification of luciferase is shown. **c,** pre-miR over-expression construct scheme. Pre-miRs hairpin (~70-110bp) were inserted downstream of an H1 promoter in a SIN lentivirus construct possessing GFP as a marker. **B. a,** Western blot of Drosha KD (DH), miR-103 OE (m103) and control (GFP) infected CaCo2 cells with (right panel) or without (left panel) 4 hours of Wnt stimulation. Axin2 protein levels are shown and quantified (upper panel). The levels of β-catenin and its phophorylated form are shown in the mid panel. Hsp90 protein levels serve as loading control. **b,** mRNA levels of Axin2 under the same treatments as **a.** were quantified by RT-qPCR.

Figure 5. Dicer depletion effects in the small intestine

A. The creation of Dicer inducible intestine epithelial cells (IECs) specific knockout mouse. $Dicer^{flox}$ mouse was crossed with a Villin Cre-ER^{T2} transgenic mouse to create conditional dicer inactivation in the gut. **B.** mRNA purified from SI crypts was used to check the relative levels of Dicer, miR-103 and mir-193a by RT-qPCR upon dicer KO (ΔDicer) or control (FL/FL). The experiment was conducted in biological duplicates. **C.** mRNA purified from SI crypts was used to check the relative levels of Paneth cell markers: Cryptdin3 and Lysozyme as in **B.**

Figure 6. Reduction of mature Paneth cells and the increment of intermediate cells

A. Lysozyme IHC assay was conducted on small intestine sections (**a,** and **b,**). Reduction of Lysozome was found in IECs Dicer depleted (ΔDicer) vs. control (FL/FL). **c, d, e,** and **f,** PAS staining of small intestine sections revealed accumulation of intermediate cells within crypts of IECs Dicer deleted (ΔDicer) vs. control (FL/FL). A larger magnification of secretory cells is shown in **e,** and **f,**. Yellow squares represent goblet cells, red circles represent Paneth cells and a combination of them represents the intermediate cells. Images were taken under 200X magnification.

Figure 7. Effects of Dicer depletion on the large intestine

A. Dicer inactivation affects normal goblet cell differentiation. **a,** Alcian blue staining of large intestine sections revealed a mass reduction in mature goblet cells in Dicer KO (ΔDicer) vs. control (FL/FL). Images were taken under 100X magnification. **b,** mRNA from LI crypts of Dicer KO (ΔDicer) and control (FL/FL) samples were analyzed by RT-qPCR for goblet cell markers (Gob5, Mucin2 and CDX-2). The RT-qPCR was conducted in biological duplicates. **c,** mRNA from LI crypts of Dicer KO (ΔDicer) and control (FL/FL) samples were analyzed by RT-qPCR for the colonocyte marker alkaline phosphatase (AP). The RT-qPCR was conducted in biological duplicates. **B.** Co-staining of alcian blue and β-catenin in LI crypts showed the accumulation of β-catenin in the nucleus (yellow arrow) and the reduction of mature goblet cells within the crypt. Minor alcian blue staining within the crypts may indicate the existence of goblet cell progenitors (red arrow). **C.** mRNA from LI crypts of Dicer KO (ΔDicer) and control (FL/FL) samples were analyzed in different stages after Tamoxifen induction (ranging from 1 to 4 weeks) by RT-qPCR for Wnt target genes, Lgr5 (GRP49) and c-Myc.

Figure 8. Immunological defects upon IEC Dicer inactivation

A. microflora analysis from stool of 1 month Dicer KO (ΔDicer) vs. control (FL/FL) revealed a spontaneous elevation in gut microflora. *Trichomona* are shown as highlight circlular shapes. **B.** mRNA from LI crypts of 1 month Dicer KO (ΔDicer) and control (FL/FL) samples were analyzed by RT-qPCR for Th2 arm effectors including IL-13, IL-4 and IL-5. The RT-qPCR was conducted

in biological duplicates. **C.** mRNA extracted from mesenteric lymph nodes (mLNs) of 6 weeks IECs Dicer KO (d), control (con), 6 weeks IECs Dicer KO infected with *T. muris* for 1 month (t-d) and control infected with *T. muris* for 1 month (t-con), was analyzed by RT-qPCR for known transcription factors of immune response, Foxp3 for Treg, GATA3 for Th2, and TBX21 for Th1. **D.** mRNA extracted from LI crypts of 6 weeks IECs Dicer KO (ΔDicer), control (FL/FL), 6 weeks IECs Dicer KO infected with *T. muris* for 1 month (Δdicer+T), and control infected with *T. muris* for 1 month (FL/FL+T), was analyzed by RT-qPCR for Th1 cytokines: IL-2, INF-γ, and TNF-α.

Figure 9. Reduction of enterocyte immunological effectors and susceptibility to *T .muris* infection

A. a, and **b,** H&E staining of Cecum of 1 month *T. muris* infected IEC Dicer KO (ΔDicer) vs. control. Pink circles represent *T. muris* anchoring to the intestine epithelium. Lack of goblet cells and epithelium damage is shown in IECs Dicer KO cecum. **c, d, e,** and **f,** RELMβ IHC of the colon. RELMβ reduction in LI sections of IECs Dicer KO (ΔDicer) vs. control (FL/FL) without *T. muris* infection (**c,** and **d,** magnification of X400) or with *T. muris* infection (**e,** and **f,** magnification of 100X). **B.** Quantification of *T. muris* worm burdens in the cecum of IECs Dicer KO (Δdicer) vs. control (FL/FL). **C.** RELMβ and TSLP mRNA levels were analyzed by RT-qPCR in LI of IECs Dicer KO (Δdicer) and control (FL/FL). The RT-qPCR was conducted in biological duplicates. **D.** RELMβ mRNA levels were analyzed by RT- qPCR in LI of 1 month *T. muris* infected mice under 6 weeks of IECs Dicer inactivation (Δdicer) and control (FL/FL). The experiment was conducted in biological duplicates. E. Protein extracted from LI crypts of 4 weeks IECs Dicer inactivated (ΔIEC), control (FL/FL), 6 weeks IECs Dicer inactivated which were infected with *T. muris* for 1 month (ΔIEC), and control infected with *T. muris* for 1 month (FL/FL+T) was analyzed by Western blot for RELMβ protein levels. Ponceau S. staining was used for loading control. Western blot was conducted in biological duplicates.

Table 1. Wnt regulated microRNAs and their predicted Wnt target genes

A bioinformatics search for Wnt regulated miRs revealed nine strong candidates (left panel). Tcf/Lef sequences within the 5kb upstream of mature miR are in the "True" column. Tcf/Lef clusters within 100bp of 5kb upstream of mature miR (max clusters column). The probability for these Tcf/Lef sequences to be found within 100bp cluster of the 5kb upstream of mature miR, is calculated with an E-value, showing a low probability for pulse positive. Axin2, a known Wnt target gene was used to set the parameters for the search. Using three different types of target prediction software, target genes that are associated with the Wnt pathway were found (right panel). Only two miRs from the search (Left panel) show no Wnt related genes as targets. The miR-103 family showed strong Wnt signaling target genes as potential candidates (red square).

Table 2. miR-30 cluster targets Sox9 3'UTR

Different miR-30 isoforms target Sox9 3'UTR, the predicted association is indicated. This association appears to be strong, probably due to a complete seed pairing (8mer) and a low thermodynamics parameters. Data retrieved from TargetScan 4 (ref).